CONVERGENCE OF A FAST EXPLICIT OPERATOR SPLITTING METHOD FOR THE EPITAXIAL GROWTH MODEL WITH SLOPE SELECTION[*]

XIAO LI[†], ZHONGHUA QIAO[‡], AND HUI ZHANG[§]

Abstract. A fast explicit operator splitting method for the epitaxial growth model with slope selection has been presented in [Cheng et al., *J. Comput. Phys.*, 303 (2015), pp. 45–65]. The original problem is split into linear and nonlinear subproblems. For the linear part, the pseudospectral method is adopted; for the nonlinear part, a 33-point difference scheme is constructed. Here, we give a compact center-difference scheme involving fewer points for the nonlinear subproblem. In addition, we analyze the convergence rate of the algorithm. The global error order $\mathcal{O}(\tau^2 + h^4)$ in discrete L^2-norm is proved theoretically and verified numerically. Some numerical experiments show the robustness of the algorithm for small coefficients of the fourth-order term for the one-dimensional case. In addition, coarsening dynamics are simulated in large domains and the 1/3 power laws are observed for the two-dimensional case.

1. Introduction. Recently, epitaxial growth has become an important technique for the growth of thin films. By using the epitaxial growth technique, it is possible to grow high-quality crystalline materials and form structures with high precision in the vertical direction [10]. There has been a large amount of research interest in the dynamics of epitaxial growth. Different kinds of models have been developed to describe the growth evolution, including atomistic models, continuum models, and hybrid models [6]. In our work, we are interested in continuum models for the evolution of epitaxial growth with slope selection [15]. Evolution is governed by the following nonlinear partial differential equation:

$$(1.1) \qquad u_t = \nabla \cdot [(|\nabla u|^2 - 1)\nabla u] - \delta \Delta^2 u, \quad (x,y) \in \Omega, \ t \in (0,T],$$

where $\delta > 0$ is a constant, $\Omega = (0, 2L)^2$ with $L > 0$, and $u : \mathbb{R}^2 \times (0, \infty) \to \mathbb{R}$ is an Ω-periodic scaled height function equipped with the initial data

$$u(x,y,0) = u_0(x,y), \quad (x,y) \in \overline{\Omega}.$$

[†]Applied and Computational Mathematics Division, Beijing Computational Science Research Center, Beijing, China, 100193 (xiaoli@csrc.ac.cn).

[‡]Corresponding author. Department of Applied Mathematics, Hong Kong Polytechnic University, Hung Hom, Kowloon, Hong Kong (zhonghua.qiao@polyu.edu.hk).

[§]Laboratory of Mathematics and Complex Systems, Ministry of Education and School of Mathematical Sciences, Beijing Normal University, Beijing 100875, People's Republic of China (hzhang@bnu.edu.cn).

The fourth-order term models the surface diffusion and the nonlinear second-order term models the Ehrlich–Schwoebel effect [5, 18, 23]. Equation (1.1) is the gradient flow with respect to the $L^2(\Omega)$ inner product of the energy functional

$$(1.2) \qquad E(u) = \int_\Omega \left(\frac{1}{4}(|\nabla u|^2 - 1)^2 + \frac{\delta}{2}|\Delta u|^2 \right) \, \mathrm{d}x\mathrm{d}y.$$

With the periodic boundary condition, it is easy to show that the energy E decreases with respect to the time. For the coarsening dynamics governed by (1.1), the exponents measured experimentally are $1/3$, which is observed in numerical simulations of the epitaxial growth [1, 22, 26, 33] and analyzed quantitively by introducing a kinetic scaling theory [15].

There have been many theoretical and numerical studies on the epitaxial growth model with slope selection. The well-posedness and regularity of the initial-boundary-value problem of the model (1.1) are studied in [15] using the Galerkin approximation method. For the growth simulations, a large computational domain is necessary in order to make the effect of periodicity assumption as small as possible and to collect enough statistical information such as mean surface height and width of the pyramid-like structures. In addition, a sufficiently long integration time is necessary in order to detect the growth behaviors and to reach the physical scaling regime. To carry out numerical simulations with large time and large computational domain, highly stable and accurate numerical schemes are required. Equation (1.1) is highly nonlinear with a small surface diffusion parameter δ, which makes it difficult to design an effective numerical scheme. In [20], two stable and convergent linearized difference schemes are derived by using the method of reduction of order [28]. The convergence rates are $\mathcal{O}(\tau + h^2)$ and $\mathcal{O}(\tau^2 + h^2)$ in discrete L^2-norm, respectively. Both the nonlinear part and the diffusion term are treated explicitly there. In [22], two unconditionally energy stable difference schemes are presented. These two schemes are second-order convergent in time and nonlinear. Because of the unconditional stability, an adaptive time-stepping strategy is proposed there. In [26, 30], the first- and second-order (in time) convex splitting schemes are constructed under the framework exploited by Eyre [7]. Still, both schemes are nonlinear and unconditionally energy stable. The similar technique has been used extensively on different phase field models, e.g., the phase field crystal models [31, 32], a diffusive interface model with the Peng–Robinson equation of state [19], etc. In [33], the authors introduce an implicit-explicit scheme combined with a Fourier pseudospectral approach, where the nonlinear term is treated explicitly and the fourth-order term implicitly. To guarantee the stability, they add an extra artificial term consistent with the truncated errors in time. However, the condition, under which the energy stability can be obtained without any restriction on time step, depends on the unknown numerical solutions. In a recent work [16], this assumption on the boundedness of the numerical solution has been removed. In [21], a mixed finite element method with the Crank–Nicolson time-stepping scheme is presented and the energy laws are proved for both semi- and fully discrete forms of the scheme.

In [1], a fast explicit operator splitting (FEOS) method based on the Strang splitting schemes [27] is constructed to simulate the model (1.1) for both one- and two-dimensional cases. The main idea of the method is to split the original equation (1.1) into nonlinear and linear parts whose exact solution operators are denoted by $\mathcal{S}_\mathcal{N}$ and $\mathcal{S}_\mathcal{L}$, and then to evolve one splitting step (from t to $t + \tau$) via three substeps:

$$u(x, y, t + \tau) = \mathcal{S}_\mathcal{L}\left(\frac{\tau}{2}\right) \mathcal{S}_\mathcal{N}(\tau) \mathcal{S}_\mathcal{L}\left(\frac{\tau}{2}\right) u(x, y, t).$$

A similar strategy has also been used to solve the phase field crystal equation in [14]. In [1], the nonlinear part is solved by the 33-point center-difference scheme combined with the large stability domain explicit Runge–Kutta solver, and the linear one by the pseudospectral method. Their numerical experiments indicate that the proper constant time step should be $\tau = \delta/100$. In addition, the FEOS method has also been successfully utilized on the convection-diffusion equations [2, 3, 4] and the modified Buckley–Leverett equations [11]. It is capable of achieving a reliable numerical solutions in an efficient manner, that is, only a few splitting steps are performed [4].

In our work, we concentrate mainly on the error estimate of the FEOS method for the model (1.1) in the two-dimensional case. The main issue, which is different from that in [1], consists of three aspects. First, we discretize the nonlinear part by a 25-point center-difference scheme in space and the explicit strong stability preserving Runge–Kutta method in time and combine the so-called frozen coefficients technique with the Fourier analysis method to derive a constraint on the time step for the stability. Second, we analyze the convergence of the entire algorithm. The global discrete L^2-error consists of the truncation errors from the splitting and the nonlinear and linear schemes, respectively. Third, we carry out numerical experiments to verify the convergence rate and test the robustness of the algorithm with small δ in the one-dimensional case. Numerical experiments suggest that the time step can be set as $\tau = \delta/10$, a little better than that in [1], because the difference scheme for nonlinear part involves fewer points, which may loosen the restriction on the time step. In addition, we simulate the two-dimensional coarsening dynamics to observe the $-1/3$ power law of the energy and the $1/3$ power law of the mean height.

The organization of this paper is as follows. In section 2, we present the FEOS method for the two-dimensional epitaxial growth model with slope selection and give a sufficient condition for the stability of the algorithm here. In section 3, the discrete L^2-error estimate of the FEOS method is shown both theoretically and numerically. Further numerical experiments are carried out and the power law for the coarsening dynamics is observed in section 4. Some concluding remarks are given in section 5.

2. Fast explicit operator splitting method. Here we present the algorithm developed in [1], where the nonlinear and linear parts are approximated by different methods, and construct a more compact difference scheme for the nonlinear part.

2.1. Splitting strategy. In [1], the model (1.1) is split into the nonlinear part

$$(2.1) \qquad u_t = \nabla \cdot (|\nabla u|^2 \nabla u) =: \mathcal{N}(u)$$

and the linear part

$$(2.2) \qquad u_t = -\Delta u - \delta \Delta^2 u,$$

whose exact solution operators are denoted by $\mathcal{S}_\mathcal{N}$ and $\mathcal{S}_\mathcal{L}$, respectively. Introducing a splitting time step τ, the solution of (1.1) is resolved from t to $t + \tau$ via the Strang splitting method [27] consisting of three substeps:

$$(2.3) \qquad u(x, y, t + \tau) = \mathcal{S}_\mathcal{L}\left(\frac{\tau}{2}\right) \mathcal{S}_\mathcal{N}(\tau) \mathcal{S}_\mathcal{L}\left(\frac{\tau}{2}\right) u(x, y, t).$$

In general, if all the solutions involved in the three-step splitting scheme (2.3) are smooth, the operator splitting method is second-order accurate [27].

For the nonlinear subproblem (2.1), the solution is L^2-stable with respect to the initial data, which is described precisely by the following proposition.

PROPOSITION 2.1. *Assuming that $u_0, v_0 \in H^2_{\mathrm{per}}(\Omega)$, we have*

$$\|\mathcal{S}_{\mathcal{N}}(t)u_0 - \mathcal{S}_{\mathcal{N}}(t)v_0\|_{L^2(\Omega)} \le \|u_0 - v_0\|_{L^2(\Omega)} \quad \forall t > 0,$$

where $H^m_{\mathrm{per}}(\Omega) = \{u|_\Omega : u \in H^m_{\mathrm{loc}}(\mathbb{R}^2) \text{ and } u \text{ is } \Omega\text{-periodic}\}$.

Proof. Set $u(x, y, t)$ and $v(x, y, t)$ to be the solutions of (2.1) with the initial data $u(\cdot, \cdot, 0) = u_0$ and $v(\cdot, \cdot, 0) = v_0$, respectively. Noting that $H^2(\Omega) \hookrightarrow W^{1,4}(\Omega)$ and using the standard Galerkin method, one could show that the solution u belongs to $C([0, T]; W^{1,4}_{\mathrm{per}}(\Omega))$ with $u_t \in L^2(0, T; L^2_{\mathrm{per}}(\Omega))$, and so does v. Let $w = u - v$; then

$$\frac{1}{2}\frac{\mathrm{d}}{\mathrm{d}t}\|w\|^2_{L^2(\Omega)} = \int_\Omega w_t w \, \mathrm{d}x\mathrm{d}y = -\int_\Omega (|\nabla u|^2 \nabla u - |\nabla v|^2 \nabla v) \cdot \nabla w \, \mathrm{d}x\mathrm{d}y$$

$$= -\frac{1}{2}\int_\Omega (|\nabla u|^2 + |\nabla v|^2 + |\nabla u + \nabla v|^2)|\nabla w|^2 \, \mathrm{d}x\mathrm{d}y \le 0,$$

which leads to $\|w(t)\|_{L^2(\Omega)} \le \|w(0)\|_{L^2(\Omega)}$, that is,

$$\|u(t) - v(t)\|_{L^2(\Omega)} \le \|u(0) - v(0)\|_{L^2(\Omega)} \quad \forall t > 0,$$

which completes the proof. $\square$

In practice, the exact solution operators $\mathcal{S}_{\mathcal{N}}$ and $\mathcal{S}_{\mathcal{L}}$ are to be replaced by their numerical approximations. In the following two subsections, we present the numerical methods given in [1], while the algorithm for the nonlinear part is a little different.

2.2. Compact center-difference scheme for the nonlinear subproblem. Using the method of lines, the nonlinear subproblem (2.1) can be reduced to a system of ODEs, which can be efficiently integrated by a stable explicit ODE solver. Here we adopt the fourth-order difference to discretize the space and choose the third-order strong stability preserving Runge–Kutta (SSP-RK3) method [8] as the ODE solver.

Introducing a spatial scale $h = 2L/J$, where $J = 2N$ is a positive even integer, the grid nodes are defined as $(x_j, y_k) = (jh, kh)$, $j, k = 1, 2, \ldots, J$. The fourth-order semidiscrete scheme for (2.1) can be written as [13]

$$(2.4) \quad \frac{\mathrm{d}u_{j,k}(t)}{\mathrm{d}t} = \frac{-F_{j+2,j,k} + 8F_{j+1,j,k} - 8F_{j-1,j,k} + F_{j-2,j,k}}{12h}$$

$$+ \frac{-G_{j,k,k+2} + 8G_{j,k,k+1} - 8G_{j,k,k-1} + G_{j,k,k-2}}{12h} =: [\mathcal{N}_h(u)]_{j,k},$$

where

$$F_{j+\ell,j,k} = F(D^\ell_x u_{j+\ell,k}, D^0_y u_{j+\ell,k}), \ G_{j,k,k+\ell} = G(D^0_x u_{j,k+\ell}, D^\ell_y u_{j,k+\ell}), \ \ell = \pm 1, \pm 2,$$

here $F(p, q) = (p^2 + q^2)p$, $G(p, q) = (p^2 + q^2)q$, and

$$(2.5a) \quad D^{+2}_x u_{j+2,k} = \frac{25u_{j+2,k} - 48u_{j+1,k} + 36u_{j,k} - 16u_{j-1,k} + 3u_{j-2,k}}{12h},$$

$$(2.5b) \quad D^{+1}_x u_{j+1,k} = \frac{3u_{j+2,k} + 10u_{j+1,k} - 18u_{j,k} + 6u_{j-1,k} - u_{j-2,k}}{12h},$$

$$(2.5c) \quad D^{-1}_x u_{j-1,k} = \frac{u_{j+2,k} - 6u_{j+1,k} + 18u_{j,k} - 10u_{j-1,k} - 3u_{j-2,k}}{12h},$$

$$(2.5d) \quad D^{-2}_x u_{j-2,k} = \frac{-3u_{j+2,k} + 16u_{j+1,k} - 36u_{j,k} + 48u_{j-1,k} - 25u_{j-2,k}}{12h},$$

$$(2.5e) \quad D^0_y u_{j+\ell,k} = \frac{-u_{j+\ell,k+2} + 8u_{j+\ell,k+1} - 8u_{j+\ell,k-1} + u_{j+\ell,k-2}}{12h}, \ \ell = \pm 1, \pm 2,$$

(2.5f) $D_x^0 u_{j,k+\ell} = \dfrac{-u_{j+2,k+\ell} + 8u_{j+1,k+\ell} - 8u_{j-1,k+\ell} + u_{j-2,k+\ell}}{12h}, \ \ell = \pm 1, \pm 2,$

(2.5g) $D_y^{+2} u_{j,k+2} = \dfrac{25u_{j,k+2} - 48u_{j,k+1} + 36u_{j,k} - 16u_{j,k-1} + 3u_{j,k-2}}{12h},$

(2.5h) $D_y^{+1} u_{j,k+1} = \dfrac{3u_{j,k+2} + 10u_{j,k+1} - 18u_{j,k} + 6u_{j,k-1} - u_{j,k-2}}{12h},$

(2.5i) $D_y^{-1} u_{j,k-1} = \dfrac{u_{j,k+2} - 6u_{j,k+1} + 18u_{j,k} - 10u_{j,k-1} - 3u_{j,k-2}}{12h},$

(2.5j) $D_y^{-2} u_{j,k-2} = \dfrac{-3u_{j,k+2} + 16u_{j,k+1} - 36u_{j,k} + 48u_{j,k-1} - 25u_{j,k-2}}{12h}.$

The fully discrete scheme for (2.1) is obtained by applying the SSP-RK3 method [8]

$$
\begin{aligned}
u^{(1)} &= u^n + \tau \mathcal{N}_h(u^n), \\
u^{(2)} &= \frac{3}{4}u^n + \frac{1}{4}u^{(1)} + \frac{1}{4}\tau \mathcal{N}_h(u^{(1)}), \\
u^{n+1} &= \frac{1}{3}u^n + \frac{2}{3}u^{(2)} + \frac{2}{3}\tau \mathcal{N}_h(u^{(2)}).
\end{aligned}
$$

(2.6)

This completes the numerical approximation of the operator $\mathcal{S_N}$. We notice that our scheme (2.4)–(2.5) is fourth-order in space, which is the same as the scheme (2.7)–(2.9) given in [1]. In addition, our scheme is more compact than the scheme in [1], since the former utilizes 25 points while the latter uses 33, as proposed in Figure 1.
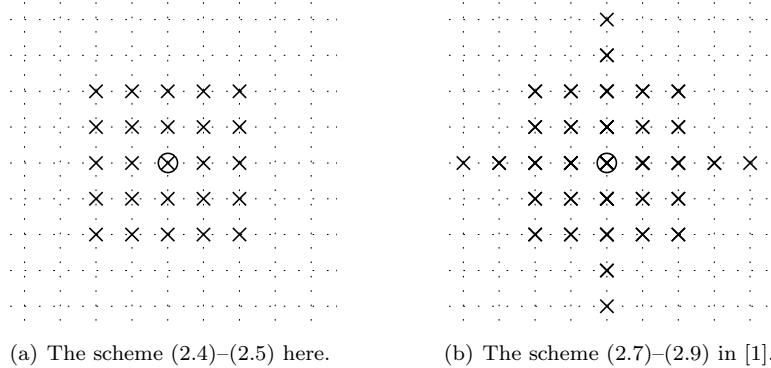

(a) The scheme (2.4)–(2.5) here.   (b) The scheme (2.7)–(2.9) in [1].

FIG. 1. *The "×" represents the point involved in the scheme expanded at the "○" point.*

According to the property of strong stability preserving, the stability restriction of the SSP-RK3 method is identical to that of the forward Euler scheme. We use the "frozen coefficients" method (see, e.g., [17]) to analyze the stability of the forward Euler scheme

(2.7) $\dfrac{u_{j,k}^{n+1} - u_{j,k}^n}{\tau} = \dfrac{-F_{j+2,j,k}^n + 8F_{j+1,j,k}^n - 8F_{j-1,j,k}^n + F_{j-2,j,k}^n}{12h}$

$\qquad\qquad\qquad + \dfrac{-G_{j,k,k+2}^n + 8G_{j,k,k+1}^n - 8G_{j,k,k-1}^n + G_{j,k,k-2}^n}{12h},$

where $F^n_{j+\ell,j,k} = F_{j+\ell,j,k}(t_n)$, $G^n_{j,k,k+\ell} = G_{j,k,k+\ell}(t_n)$, $\ell = \pm 1, \pm 2$, that is,

$$
\frac{u^{n+1}_{j,k} - u^n_{j,k}}{\tau} = (|\nabla_h u|^2)^n_{j+2,j,k} \cdot \left[-\frac{D^{+2}_x u^n_{j+2,k}}{12h} \right] + (|\nabla_h u|^2)^n_{j+1,j,k} \cdot \left[\frac{2D^{+1}_x u^n_{j+1,k}}{3h} \right]
$$
$$
+ (|\nabla_h u|^2)^n_{j-1,j,k} \cdot \left[-\frac{2D^{-1}_x u^n_{j-1,k}}{3h} \right] + (|\nabla_h u|^2)^n_{j-2,j,k} \cdot \left[\frac{D^{-2}_x u^n_{j-2,k}}{12h} \right]
$$
$$
+ (|\nabla_h u|^2)^n_{j,k,k+2} \cdot \left[-\frac{D^{+2}_y u^n_{j,k+2}}{12h} \right] + (|\nabla_h u|^2)^n_{j,k,k+1} \cdot \left[\frac{2D^{+1}_y u^n_{j,k+1}}{3h} \right]
$$
$$
+ (|\nabla_h u|^2)^n_{j,k,k-1} \cdot \left[-\frac{2D^{-1}_y u^n_{j,k-1}}{3h} \right] + (|\nabla_h u|^2)^n_{j,k,k-2} \cdot \left[\frac{D^{-2}_y u^n_{j,k-2}}{12h} \right],
$$

where

$$
(|\nabla_h u|^2)^n_{j+\ell,j,k} = (D^\ell_x u^n_{j+\ell,k})^2 + (D^0_y u^n_{j+\ell,k})^2,
$$
$$
(|\nabla_h u|^2)^n_{j,k,k+\ell} = (D^0_x u^n_{j,k+\ell})^2 + (D^\ell_y u^n_{j,k+\ell})^2.
$$

The terms $D^\ell_x u^n_{j+\ell,k}$, $D^0_y u^n_{j+\ell,k}$, $D^0_x u^n_{j,k+\ell}$, $D^\ell_y u^n_{j,k+\ell}$ approximate the values $u_x(x_{j+\ell}, y_k, t_n)$, $u_y(x_{j+\ell}, y_k, t_n)$, $u_x(x_j, y_{k+\ell}, t_n)$, $u_y(x_j, y_{k+\ell}, t_n)$ with the error $\mathcal{O}(h^4)$, respectively. Freezing the prefactors of the square bracket terms by the constant

$$
A := \max_{j,k}\{(|\nabla_h u|^2)^n_{j+\ell,j,k}, (|\nabla_h u|^2)^n_{j,k,k+\ell} : \ell = \pm 1, \pm 2\},
$$

we obtain the following linear scheme:

$$
\frac{u^{n+1}_{j,k} - u^n_{j,k}}{\tau} = A \cdot \left(\frac{-u^n_{j+2,k} + 16u^n_{j+1,k} - 30u^n_{j,k} + 16u^n_{j-1,k} - u^n_{j-2,k}}{12h^2} \right.
$$
$$
\left. + \frac{-u^n_{j,k+2} + 16u^n_{j,k+1} - 30u^n_{j,k} + 16u^n_{j,k-1} - u^n_{j,k-2}}{12h^2} \right),
$$

which can be transformed into the following form:

$$
(2.8) \qquad u^{n+1}_{j,k} = (1 - 5r)u^n_{j,k} + \frac{4r}{3}(u^n_{j+1,k} + u^n_{j-1,k} + u^n_{j,k+1} + u^n_{j,k-1})
$$
$$
- \frac{r}{12}(u^n_{j+2,k} + u^n_{j-2,k} + u^n_{j,k+2} + u^n_{j,k-2}),
$$

where $r = A\tau/h^2$. The "frozen coefficients" method says that (2.7) is (locally) discrete L^2-stable as long as (2.8) is discrete L^2-stable. Using the Fourier analysis method, the symbol of the difference scheme (2.8) is

$$
\rho(\sigma_1, \sigma_2) = 1 - \frac{r}{3}[(1 - \cos\sigma_1 h)(7 - \cos\sigma_1 h) + (1 - \cos\sigma_2 h)(7 - \cos\sigma_2 h)].
$$

Therefore, $|\rho(\sigma_1, \sigma_2)| \le 1$ if and only if

$$
0 \le r \le \frac{6}{(1 - \cos\sigma_1 h)(7 - \cos\sigma_1 h) + (1 - \cos\sigma_2 h)(7 - \cos\sigma_2 h)}.
$$

As $(1 - c)(7 - c) \in [0, 16]$ when $c \in [-1, 1]$, we obtain $r \le \frac{3}{16}$, namely,

$$
(2.9) \qquad \tau \le \frac{3}{16A}h^2.
$$

Obviously, this is a sufficient but not necessary condition for the stability of the Euler scheme (2.7) and thus of the scheme (2.4) combined with the SSP-RK3 solver.

2.3. Pseudospectral method for the linear subproblem. In [1], (2.2) is solved by the pseudospectral method via the following procedure. They first use the FFT algorithm to compute the discrete Fourier coefficients $\{\widetilde{u}_{pq}(t)\}$ from the point values $\{u_{j,k}(t)\}$. Then they calculate $\widetilde{u}_{pq}(t+\tau) = \mathrm{e}^{\lambda_{pq}\tau}\widetilde{u}_{pq}(t)$, where

$$\lambda_{pq} = \frac{\pi^2(p^2+q^2)}{L^2} - \delta\left(\frac{\pi^2(p^2+q^2)}{L^2}\right)^2.$$

Finally they recover the point values of the solution at the new time level, $\{u_{j,k}(t+\tau)\}$, from the discrete Fourier coefficients $\{\widetilde{u}_{pq}(t+\tau)\}$ using the inverse FFT algorithm.

For the continuous and Ω-periodic function $u(x,y,t)$, there exists the Fourier series in the complex form at time t:

$$(2.10) \qquad u(x,y,t) = \sum_{p=-\infty}^{\infty} \sum_{q=-\infty}^{\infty} \widehat{u}_{pq}(t)\mathrm{e}^{\frac{\mathrm{i}\pi}{L}(px+qy)},$$

where the Fourier coefficients are given by

$$(2.11) \qquad \widehat{u}_{pq}(t) = \frac{1}{4L^2}\int_\Omega u(x,y,t)\mathrm{e}^{-\frac{\mathrm{i}\pi}{L}(px+qy)}\,\mathrm{d}x\mathrm{d}y, \quad p,q = 0,\pm 1,\pm 2,\ldots.$$

It is easy to see that the Fourier coefficients satisfy the following ODEs:

$$\frac{\mathrm{d}}{\mathrm{d}t}\widehat{u}_{pq}(t) = \lambda_{pq}\widehat{u}_{pq}(t), \quad \lambda_{pq} = \frac{\pi^2(p^2+q^2)}{L^2} - \delta\left(\frac{\pi^2(p^2+q^2)}{L^2}\right)^2.$$

The exact solution is

$$\widehat{u}_{pq}(t+\tau) = \mathrm{e}^{\lambda_{pq}\tau}\widehat{u}_{pq}(t), \quad p,q = 0,\pm 1,\pm 2,\ldots,$$

and then

$$(2.12) \qquad u(x,y,t+\tau) = \sum_{p=-\infty}^{\infty} \sum_{q=-\infty}^{\infty} \widehat{u}_{pq}(t+\tau)\mathrm{e}^{\frac{\mathrm{i}\pi}{L}(px+qy)}.$$

It is easy to see that the pseudospectral method proposed in [1] is the discrete form of the procedure above.

In the theory of the spectral method [24, 25], the FFT and the inverse FFT algorithm can be expressed as

$$(2.13) \quad \widetilde{u}_{pq}(t) = \frac{1}{J^2 c_p c_q}\sum_{j=1}^{J}\sum_{k=1}^{J} u(x_j,y_k,t)\mathrm{e}^{-\frac{\mathrm{i}\pi}{L}(px_j+qy_k)}, \quad p,q = 0,\pm 1,\pm 2,\ldots,\pm N,$$

and

$$(2.14) \qquad u_{j,k}(t) = \sum_{p=-N}^{N}\sum_{q=-N}^{N} \widetilde{u}_{pq}(t)\mathrm{e}^{\frac{\mathrm{i}\pi}{L}(px_j+qy_k)}, \quad j,k = 1,2,\ldots,J,$$

where c_p and c_q are defined as

$$(2.15) \qquad c_r = \begin{cases} 2, & |r| = N, \\ 1, & |r| < N. \end{cases}$$

The pseudospectral procedure can be expressed as

$$u(t + \tau) = \mathscr{F}_d^{-1}\{e^{\lambda_{pq}\tau}\mathscr{F}_d[u(t)](p, q)\},$$

where $u(t)$ is the matrix with the elements $\{u_{j,k}(t) : j, k = 1, 2, \ldots, J\}$, and $\mathscr{F}_d$ and $\mathscr{F}_d^{-1}$ are the discrete Fourier transform and the inverse transform, respectively. Using the Parseval's formula and the fact that $|e^{\lambda_{pq}\tau}| \leq e^{\frac{\tau}{4\delta}}$ (for any p, q), we obtain

$$(2.16) \qquad \|u(t + \tau)\| \leq e^{\frac{\tau}{4\delta}}\|u(t)\|,$$

where $\|\cdot\|$ represents the discrete L^2-norm, that is,

$$\|u\| = \sqrt{h^2 \sum_{j=1}^{J} \sum_{k=1}^{J}(u_{j,k})^2}.$$

The inequality (2.16) implies the stability of the pseudospectral procedure.

Remark 2.2. We point out that we just consider the L^2-stability rather than energy stability of the numerical solutions. In fact, such a splitting scheme as (2.3) cannot preserve the energy stability as the original problem (1.1).

3. Error analysis and accuracy tests. Here we investigate the convergence rate of the FEOS method given above, and then conduct some numerical accuracy tests to verify our results. It is well-known that the spatial size h is usually controlled as order $\mathcal{O}(\sqrt{\delta})$ in order to capture the interfaces, that is, $h \leq C_{11}\sqrt{\delta}$ for some $C_{11} > 0$. Combining with the stability condition (2.9), we have

$$(3.1) \qquad \tau \leq \frac{3C_{11}^2}{16A}\delta.$$

3.1. Error estimate. We denote by $\widetilde{u}(x, y, t)$ the splitting solution satisfying exactly the scheme (2.3) and write $U_{jk}^n := u(x_j, y_k, t_n)$, $\widetilde{u}^n := \widetilde{u}(\cdot, \cdot, t_n)$, and $\widetilde{U}_{jk}^n := \widetilde{u}(x_j, y_k, t_n)$. We denote by $\mathcal{S}_{\mathcal{N}}^h$ and $\mathcal{S}_{\mathcal{L}}^h$ the discrete approximations of the operators $\mathcal{S}_{\mathcal{N}}$ and $\mathcal{S}_{\mathcal{L}}$, respectively, and by u_{jk}^n the numerical approximation of $\widetilde{U}_{jk}^n$, satisfying

$$u^{n+1} = \mathcal{S}_{\mathcal{L}}^h\left(\frac{\tau}{2}\right)\mathcal{S}_{\mathcal{N}}^h(\tau)\mathcal{S}_{\mathcal{L}}^h\left(\frac{\tau}{2}\right)u^n.$$

Defining a sample operator $I^h : C_{\mathrm{per}}^0(\overline{\Omega}) \to \mathbb{R}^{J \times J}$ as $I^h u = (u(x_j, y_k))_{jk}$, we have $\widetilde{U}^n = I^h \widetilde{u}^n$, where $C_{\mathrm{per}}^m(\overline{\Omega}) = \{u|_{\overline{\Omega}} : u \in C^m(\mathbb{R}^2) \text{ and } u \text{ is } \Omega\text{-periodic}\}$. For simple notation, we omit the $\frac{\tau}{2}$ or τ following the symbols $\mathcal{S}_{\mathcal{N}}$, $\mathcal{S}_{\mathcal{L}}$, $\mathcal{S}_{\mathcal{N}}^h$, or $\mathcal{S}_{\mathcal{L}}^h$ below.

To estimate the error, we need some lemmas. For simplicity, we write $\mathcal{S}_{\mathcal{N}}u$ to mean $\mathcal{S}_{\mathcal{N}}(u)$ and $\mathcal{S}_{\mathcal{N}}^h v$ to mean $\mathcal{S}_{\mathcal{N}}^h(v)$, though the operators $\mathcal{S}_{\mathcal{N}}$ and $\mathcal{S}_{\mathcal{N}}^h$ are actually nonlinear. We state the accuracy of $\mathcal{S}_{\mathcal{N}}^h$ obtained in section 2.2.

LEMMA 3.1. *Assume that the solution to the nonlinear subproblem* (2.1) *belongs to* $H^5(0, T; H_{\mathrm{per}}^8(\Omega))$. *Under the condition* (3.1), *there exists a positive constant* C_1, *independent on* τ *and* h, *such that*

$$\|I^h\mathcal{S}_{\mathcal{N}}u - \mathcal{S}_{\mathcal{N}}^h I^h u\| \leq C_1\tau(\tau^3 + h^4) \quad \forall u \in H_{\mathrm{per}}^8(\Omega).$$

Proof. To avoid confusing notation, we denote by $V(x, y, t)$ the exact solution to the subproblem (2.1) and by $v_{j,k}^n$ the numerical solution approximating

$V_{j,k}^n := V(x_j, y_k, t_n)$. Our purpose is to estimate $\|V^{n+1} - v^{n+1}\|$ provided $V_{j,k}^n = v_{j,k}^n = u(x_j, y_k)$ for given $u \in C_{\mathrm{per}}^6(\overline{\Omega})$. Recall that the numerical solution v^{n+1} satisfies

$$
\begin{aligned}
v^{(1)} &= v^n + \tau \mathcal{N}_h(v^n), \\
v^{(2)} &= \frac{3}{4} v^n + \frac{1}{4} v^{(1)} + \frac{1}{4} \tau \mathcal{N}_h(v^{(1)}), \\
v^{n+1} &= \frac{1}{3} v^n + \frac{2}{3} v^{(2)} + \frac{2}{3} \tau \mathcal{N}_h(v^{(2)}),
\end{aligned}
$$

and correspondingly, the exact solution V^{n+1} satisfies

$$
\begin{aligned}
V^{(1)} &= V^n + \tau (\mathcal{N}_h(V^n) + R_h^n), \\
V^{(2)} &= \frac{3}{4} V^n + \frac{1}{4} V^{(1)} + \frac{1}{4} \tau (\mathcal{N}_h(V^{(1)}) + R_h^{(1)}), \\
V^{n+1} &= \frac{1}{3} V^n + \frac{2}{3} V^{(2)} + \frac{2}{3} \tau (\mathcal{N}_h(V^{(2)}) + R_h^{(2)}) + R_\tau^{n+1},
\end{aligned}
$$

where R_τ^{n+1} is the truncated error generated by using the SSP-RK3 solver, and

$$
R_h^n := \mathcal{N}(V^n) - \mathcal{N}_h(V^n), \quad R_h^{(1)} := \mathcal{N}(V^{(1)}) - \mathcal{N}_h(V^{(1)}), \quad R_h^{(2)} := \mathcal{N}(V^{(2)}) - \mathcal{N}_h(V^{(2)}).
$$

Generally, we denote $R_h = \mathcal{N}(V) - \mathcal{N}_h(V)$. Using the Taylor formula, we have

$$
\begin{aligned}
R_h = &-\frac{2h^4}{5}(|\nabla V|^2 V_x^{(5)})_x + \frac{h^4}{15}(V_x V_y V_y^{(5)})_x + \frac{h^4}{30}(|\nabla V|^2 V_x)_x^{(5)} \\
&-\frac{2h^4}{5}(|\nabla V|^2 V_y^{(5)})_y + \frac{h^4}{15}(V_x V_y V_x^{(5)})_y + \frac{h^4}{30}(|\nabla V|^2 V_y)_y^{(5)} + \text{h.o.t.}
\end{aligned}
$$

If $V \in C^4([0,T]; C_{\mathrm{per}}^6(\overline{\Omega}))$, we have $\|R_h\| \leq C' h^4$ and $\|R_\tau^{n+1}\| \leq C'' \tau^4$. By noting that the mapping $\mathcal{N}_h : \mathbb{R}^{J \times J} \to \mathbb{R}^{J \times J}$ is an elementary function, we know that the Jacobian of $\mathcal{N}_h$ is bounded by a constant, denoted by K, and then $\mathcal{N}_h$ is Lipschitz continuous with K the Lipschitz constant. Since

$$
\begin{aligned}
V^{(1)} - v^{(1)} &= \tau R_h^n, \\
V^{(2)} - v^{(2)} &= \frac{1}{4}(V^{(1)} - v^{(1)}) + \frac{1}{4}\tau(\mathcal{N}_h(V^{(1)}) - \mathcal{N}_h(v^{(1)})) + \frac{1}{4}\tau R_h^{(1)}, \\
V^{n+1} - v^{n+1} &= \frac{2}{3}(V^{(2)} - v^{(2)}) + \frac{2}{3}\tau(\mathcal{N}_h(V^{(2)}) - \mathcal{N}_h(v^{(2)})) + \frac{2}{3}\tau R_h^{(2)} + R_\tau^{n+1},
\end{aligned}
$$

we obtain

$$
\begin{aligned}
\|V^{(1)} - v^{(1)}\| &= \tau \|R_h^n\| \leq C' \tau h^4, \\
\|V^{(2)} - v^{(2)}\| &\leq \frac{1}{4}(1 + K\tau)\|V^{(1)} - v^{(1)}\| + \frac{1}{4}\tau \|R_h^{(1)}\| \\
&\leq \frac{1}{4}C'(1 + K\tau)\tau h^4 + \frac{1}{4}C'\tau h^4 = \frac{1}{4}C'(2 + K\tau)\tau h^4, \\
\|V^{n+1} - v^{n+1}\| &\leq \frac{2}{3}(1 + K\tau)\|V^{(2)} - v^{(2)}\| + \frac{2}{3}\tau \|R_h^{(2)}\| + \|R_\tau^{n+1}\| \\
&\leq \frac{1}{6}C'(1 + K\tau)(2 + K\tau)\tau h^4 + \frac{2}{3}C'\tau h^4 + C''\tau^4.
\end{aligned}
$$

Under the condition (3.1), we have

$$\|V^{n+1} - v^{n+1}\| \le C_1(\tau h^4 + \tau^4).$$

According to the Sobolev embedding theorem, we have

$$H^8_{\mathrm{per}}(\Omega) \hookrightarrow C^6_{\mathrm{per}}(\overline{\Omega}), \quad H^5(0,T; H^8_{\mathrm{per}}(\Omega)) \hookrightarrow C^4([0,T]; C^6_{\mathrm{per}}(\overline{\Omega})),$$

which completes the proof. □

We can derive the stability of $\mathcal{S}_{\mathcal{N}}^h$ by using the result of $\mathcal{S}_{\mathcal{N}}$.

LEMMA 3.2. *Given $m \ge 8$. Under the condition* (3.1), *there exists a positive constant C_2, independent on τ and h, such that*

$$\|\mathcal{S}_{\mathcal{N}}^h v - \mathcal{S}_{\mathcal{N}}^h w\| \le \|v - w\| + 2C_1\tau(\tau^3 + h^4) + C_2 h^m \quad \forall v, w \in \mathbb{R}^{J \times J}.$$

Proof. Let $\overline{v}$ be some function, belonging to $H^m_{\mathrm{per}}(\Omega)$, such that $I^h \overline{v} = v$, for example, the two-dimensional trigonometric interpolation of v in Ω. Similarly, let $\overline{w} \in H^m_{\mathrm{per}}(\Omega)$ such that $I^h \overline{w} = w$. Using Lemma 3.1, we obtain

$$\begin{aligned}\|\mathcal{S}_{\mathcal{N}}^h v - \mathcal{S}_{\mathcal{N}}^h w\| &\le \|\mathcal{S}_{\mathcal{N}}^h v - I^h \mathcal{S}_{\mathcal{N}} \overline{v}\| + \|I^h \mathcal{S}_{\mathcal{N}} \overline{v} - I^h \mathcal{S}_{\mathcal{N}} \overline{w}\| + \|I^h \mathcal{S}_{\mathcal{N}} \overline{w} - \mathcal{S}_{\mathcal{N}}^h w\| \\ &\le C_1\tau(\tau^3 + h^4) + \|I^h(\mathcal{S}_{\mathcal{N}} \overline{v} - \mathcal{S}_{\mathcal{N}} \overline{w})\| + C_1\tau(\tau^3 + h^4).\end{aligned}$$

Since the L^2-norm of an Ω-periodic function on Ω can be approximated by the discrete L^2-norm with spectral accuracy [29], using Proposition 2.1, we have

$$\begin{aligned}\|I^h(\mathcal{S}_{\mathcal{N}} \overline{v} - \mathcal{S}_{\mathcal{N}} \overline{w})\| &\le \|\mathcal{S}_{\mathcal{N}} \overline{v} - \mathcal{S}_{\mathcal{N}} \overline{w}\|_{L^2(\Omega)} + Ch^m \\ &\le \|\overline{v} - \overline{w}\|_{L^2(\Omega)} + Ch^m \le \|v - w\| + C_2 h^m.\end{aligned}$$

Therefore, we obtain

$$\|\mathcal{S}_{\mathcal{N}}^h v - \mathcal{S}_{\mathcal{N}}^h w\| \le \|v - w\| + 2C_1\tau(\tau^3 + h^4) + C_2 h^m,$$

which completes the proof. □

The stability inequality (2.16) can be rewritten in the following form.

LEMMA 3.3. $\|\mathcal{S}_{\mathcal{L}}^h v\| \le \mathrm{e}^{\frac{\tau}{4\delta}}\|v\| \ \forall v \in \mathbb{R}^{J \times J}.$

The error estimate of the operator $\mathcal{S}_{\mathcal{L}}^h$ defined in section 2.3 can be proved in the framework of a spectral method [25] (see also [9]).

LEMMA 3.4. *Given $m \in \mathbb{N}$ and $m > 1$, there exists a positive constant C_3, independent on τ and h, such that*

$$\|I^h \mathcal{S}_{\mathcal{L}} u - \mathcal{S}_{\mathcal{L}}^h I^h u\| \le C_3 |u|_m \mathrm{e}^{\frac{\tau}{4\delta}} h^m \quad \forall u \in H^m_{\mathrm{per}}(\Omega).$$

Proof. We use the notation w, $\overline{w}$, $\widehat{w}$, and $\widetilde{w}$, representing

$$w(x,y,t) = \sum_{p=-\infty}^{\infty}\sum_{q=-\infty}^{\infty} \widehat{u}_{pq}(t)\mathrm{e}^{\frac{\mathrm{i}\pi}{L}(px+qy)}, \quad \overline{w}(x,y,t) = \sum_{p=-\infty}^{\infty}\sum_{q=-N}^{N} \widehat{u}_{pq}(t)\mathrm{e}^{\frac{\mathrm{i}\pi}{L}(px+qy)},$$

$$\widehat{w}(x,y,t) = \sum_{p=-N}^{N}\sum_{q=-N}^{N} \widehat{u}_{pq}(t)\mathrm{e}^{\frac{\mathrm{i}\pi}{L}(px+qy)}, \quad \widetilde{w}(x,y,t) = \sum_{p=-N}^{N}\sum_{q=-N}^{N} \widetilde{u}_{pq}(t)\mathrm{e}^{\frac{\mathrm{i}\pi}{L}(px+qy)},$$

where $\widehat{u}_{pq}(t)$ and $\widetilde{u}_{pq}(t)$ are given by (2.11) and (2.13), respectively, Assuming that $w(\cdot,\cdot,0) = \overline{w}(\cdot,\cdot,0) = \widehat{w}(\cdot,\cdot,0) = \widetilde{w}(\cdot,\cdot,0) = u$, we know that

$$\|I^h \mathcal{S}_{\mathcal{L}} u - \mathcal{S}_{\mathcal{L}}^h I^h u\|^2 = h^2 \sum_{j=1}^{2N} \sum_{k=1}^{2N} |w(x_j, y_k, \tau) - \widetilde{w}(x_j, y_k, \tau)|^2 \le 4A_1 + 4A_2 + 2B,$$

where

$$A_1 = h^2 \sum_{j=1}^{2N} \sum_{k=1}^{2N} |w(x_j, y_k, \tau) - \overline{w}(x_j, y_k, \tau)|^2,$$

$$A_2 = h^2 \sum_{j=1}^{2N} \sum_{k=1}^{2N} |\overline{w}(x_j, y_k, \tau) - \widehat{w}(x_j, y_k, \tau)|^2,$$

$$B = h^2 \sum_{j=1}^{2N} \sum_{k=1}^{2N} |\widehat{w}(x_j, y_k, \tau) - \widetilde{w}(x_j, y_k, \tau)|^2.$$

We first estimate the terms A_1 and A_2. Since

$$A_1 = h^2 \sum_{j=1}^{2N} \sum_{k=1}^{2N} \left| \sum_{p=-\infty}^{\infty} \sum_{|q|>N} \widehat{u}_{pq}(\tau) e^{\frac{i\pi}{L}(px_j + qy_k)} \right|^2$$

$$= 4L^2 \sum_{p=-\infty}^{\infty} \sum_{|q|>N} |\widehat{u}_{pq}(\tau)|^2$$

$$\le 4L^2 e^{\frac{\tau}{2\delta}} \sum_{p=-\infty}^{\infty} \sum_{|q|>N} |\widehat{u}_{pq}(0)|^2$$

$$\le 4L^2 e^{\frac{\tau}{2\delta}} \sum_{p=-\infty}^{\infty} \left(N^{-2m} \sum_{|q|>N} q^{2m} |\widehat{u}_{pq}(0)|^2 \right)$$

$$= 4L^2 e^{\frac{\tau}{2\delta}} N^{-2m} \sum_{p=-\infty}^{\infty} \sum_{|q|>N} q^{2m} |\widehat{u}_{pq}(0)|^2,$$

and, similarly,

$$A_2 = h^2 \sum_{j=1}^{2N} \sum_{k=1}^{2N} \left| \sum_{q=-N}^{N} \sum_{|p|>N} \widehat{u}_{pq}(\tau) e^{\frac{i\pi}{L}(px_j + qy_k)} \right|^2$$

$$\le 4L^2 e^{\frac{\tau}{2\delta}} N^{-2m} \sum_{q=-N}^{N} \sum_{|p|>N} p^{2m} |\widehat{u}_{pq}(0)|^2,$$

we obtain

$$A_1 + A_2 \le 4L^2 e^{\frac{\tau}{2\delta}} N^{-2m} \left(\sum_{p=-\infty}^{\infty} \sum_{|q|>N} q^{2m} |\widehat{u}_{pq}(0)|^2 + \sum_{q=-N}^{N} \sum_{|p|>N} p^{2m} |\widehat{u}_{pq}(0)|^2 \right)$$

$$\le 4L^2 e^{\frac{\tau}{2\delta}} N^{-2m} \sum_{p=-\infty}^{\infty} \sum_{q=-\infty}^{\infty} (p^{2m} + q^{2m}) |\widehat{u}_{pq}(0)|^2$$

$$\leq 4L^2 \mathrm{e}^{\frac{\tau}{2\delta}} N^{-2m} \sum_{p=-\infty}^{\infty} \sum_{q=-\infty}^{\infty} (p^2+q^2)^m |\widehat{u}_{pq}(0)|^2$$

$$= 4L^2 \mathrm{e}^{\frac{\tau}{2\delta}} N^{-2m} |u|_m^2,$$

where $|\cdot|_m$ represents the seminorm of $H_{\mathrm{per}}^m(\Omega)$.

We next estimate the term B. It is easy to obtain

$$B = h^2 \sum_{j=1}^{2N} \sum_{k=1}^{2N} \left| \sum_{p=-N}^{N} \sum_{q=-N}^{N} (\widehat{u}_{pq}(\tau) - \widetilde{u}_{pq}(\tau)) \mathrm{e}^{\frac{\mathrm{i}\pi}{L}(px+qy)} \right|^2$$

$$= 4L^2 \sum_{p=-N}^{N} \sum_{q=-N}^{N} |\widehat{u}_{pq}(\tau) - \widetilde{u}_{pq}(\tau)|^2$$

$$\leq 4L^2 \mathrm{e}^{\frac{\tau}{2\delta}} \sum_{p=-N}^{N} \sum_{q=-N}^{N} |\widehat{u}_{pq}(0) - \widetilde{u}_{pq}(0)|^2.$$

Now we look for the upper bound of B via the following four steps.

(i) Magnify the sum

$$D := \sum_{p=-N}^{N} \sum_{q=-N}^{N} |\widehat{u}_{pq} - \widetilde{u}_{pq}|^2.$$

A direct calculation leads to

$$D = \sum_{p=-N}^{N} \left(\sum_{q=-N+1}^{N-1} |\widehat{u}_{pq} - \widetilde{u}_{pq}|^2 + \frac{1}{4} \sum_{q=\pm N} |2\widehat{u}_{pq} - 2\widetilde{u}_{pq}|^2 \right)$$

$$\leq \sum_{p=-N}^{N} \left(\sum_{q=-N+1}^{N-1} |\widehat{u}_{pq} - \widetilde{u}_{pq}|^2 + \frac{1}{2} \sum_{q=\pm N} |\widehat{u}_{pq} - 2\widetilde{u}_{pq}|^2 + \frac{1}{2} \sum_{q=\pm N} |\widehat{u}_{pq}|^2 \right)$$

$$\leq \sum_{p=-N}^{N} \left(\sum_{q=-N}^{N} |\widehat{u}_{pq} - c_q \widetilde{u}_{pq}|^2 + \frac{1}{2} \sum_{q=\pm N} |\widehat{u}_{pq}|^2 \right)$$

$$= \sum_{q=-N}^{N} \left(\sum_{p=-N}^{N} |\widehat{u}_{pq} - c_q \widetilde{u}_{pq}|^2 \right) + \frac{1}{2} \sum_{p=-N}^{N} \sum_{q=\pm N} |\widehat{u}_{pq}|^2$$

$$\leq \sum_{q=-N}^{N} \left(\sum_{p=-N}^{N} |\widehat{u}_{pq} - c_p c_q \widetilde{u}_{pq}|^2 + \frac{1}{2} \sum_{p=\pm N} |\widehat{u}_{pq}|^2 \right) + \frac{1}{2} \sum_{p=-N}^{N} \sum_{q=\pm N} |\widehat{u}_{pq}|^2$$

$$= \sum_{p=-N}^{N} \sum_{q=-N}^{N} |\widehat{u}_{pq} - c_p c_q \widetilde{u}_{pq}|^2 + \frac{1}{2} \sum_{q=-N}^{N} \sum_{p=\pm N} |\widehat{u}_{pq}|^2 + \frac{1}{2} \sum_{p=-N}^{N} \sum_{q=\pm N} |\widehat{u}_{pq}|^2$$

$$=: D_1 + D_2 + D_3,$$

where c_p and c_q are defined as in (2.15).

(ii) Estimate the term $D_2 + D_3$. Since

$$D_2 = \frac{1}{2} \sum_{q=-N}^{N} \sum_{p=\pm N} |\widehat{u}_{pq}|^2 \leq \frac{1}{2} \sum_{q=-N}^{N} \left(N^{-2m} \sum_{|p| \geq N} p^{2m} |\widehat{u}_{pq}|^2 \right)$$

$$= \frac{1}{2}N^{-2m}\sum_{q=-N}^{N}\sum_{|p|\geq N}p^{2m}|\widehat{u}_{pq}|^2 \leq \frac{1}{2}N^{-2m}\sum_{q=-\infty}^{\infty}\sum_{p=-\infty}^{\infty}p^{2m}|\widehat{u}_{pq}|^2,$$

and, similarly,

$$D_3 \leq \frac{1}{2}N^{-2m}\sum_{p=-\infty}^{\infty}\sum_{q=-\infty}^{\infty}q^{2m}|\widehat{u}_{pq}|^2,$$

we obtain

$$D_2 + D_3 \leq \frac{1}{2}N^{-2m}\sum_{q=-\infty}^{\infty}\sum_{p=-\infty}^{\infty}(p^2+q^2)^m|\widehat{u}_{pq}|^2 = \frac{1}{2}N^{-2m}|u|_m^2.$$

(iii) To estimate the term D_1, we first prove that

(3.2) $$c_p c_q \widetilde{u}_{pq} = \widehat{u}_{pq} + \sum_{r^2+s^2\neq 0}\widehat{u}_{p+2rN,q+2sN}.$$

In fact, substituting (2.10) into (2.13), we have

$$c_p c_q \widetilde{u}_{pq} = \frac{1}{4N^2}\sum_{j=1}^{2N}\sum_{k=1}^{2N}\left(\sum_{r=-\infty}^{\infty}\sum_{s=-\infty}^{\infty}\widehat{u}_{rs}e^{\frac{i\pi}{L}(rx_j+sy_k)}\right)e^{-\frac{i\pi}{L}(px_j+qy_k)}$$

$$= \frac{1}{4N^2}\sum_{j=1}^{2N}\sum_{k=1}^{2N}\sum_{r=-\infty}^{\infty}\sum_{s=-\infty}^{\infty}\widehat{u}_{rs}e^{\frac{i\pi}{L}((r-p)x_j+(s-q)y_k)}$$

$$= \frac{1}{4N^2}\sum_{r=-\infty}^{\infty}\sum_{s=-\infty}^{\infty}\widehat{u}_{rs}\sum_{j=1}^{2N}e^{\frac{i\pi}{L}(r-p)x_j}\sum_{k=1}^{2N}e^{\frac{i\pi}{L}(s-q)y_k}$$

$$= \sum_{r=-\infty}^{\infty}\sum_{s=-\infty}^{\infty}\widehat{u}_{p+2rN,q+2sN}$$

$$= \widehat{u}_{pq} + \sum_{r^2+s^2\neq 0}\widehat{u}_{p+2rN,q+2sN},$$

since

$$\sum_{j=1}^{2N}e^{\frac{i\pi}{L}(r-p)x_j} = \begin{cases}2N, & r-p=2lN,\\ 0, & r-p\neq 2lN,\end{cases} \quad \text{here } l \text{ is an integer.}$$

(iv) Estimate the term D_1. Using the formula (3.2) and the Cauchy–Schwarz inequality, we have

$$D_1 = \sum_{p=-N}^{N}\sum_{q=-N}^{N}\left|\sum_{r^2+s^2\neq 0}\widehat{u}_{p+2rN,q+2sN}\right|^2$$

$$\leq \sum_{p=-N}^{N}\sum_{q=-N}^{N}\left\{\left(\sum_{r^2+s^2\neq 0}\left[(p+2rN)^2+(q+2sN)^2\right]^{-m}\right)\cdot\right.$$

$$\left.\left(\sum_{r^2+s^2\neq 0}\left[(p+2rN)^2+(q+2sN)^2\right]^{m}|\widehat{u}_{p+2rN,q+2sN}|^2\right)\right\}$$

$$\leq \max_{|p|,|q|\leq N} \left(\sum_{r^2+s^2\neq 0} \left[(p+2rN)^2 + (q+2sN)^2 \right]^{-m} \right) \cdot$$

$$\left(\sum_{p=-N}^{N} \sum_{q=-N}^{N} \sum_{r^2+s^2\neq 0} \left[(p+2rN)^2 + (q+2sN)^2 \right]^m |\widehat{u}_{p+2rN,q+2sN}|^2 \right)$$

$$\leq \left(\sum_{r^2+s^2\neq 0} \left[(2rN-N)^2 + (2sN-N)^2 \right]^{-m} \right) \cdot 2|u|_m^2$$

$$= 2N^{-2m}|u|_m^2 \sum_{r^2+s^2\neq 0} \frac{1}{\left[(2r-1)^2+(2s-1)^2\right]^m}.$$

The series

$$\sum_{r^2+s^2\neq 0} \frac{1}{\left[(2r-1)^2+(2s-1)^2\right]^m} \leq \sum_{r^2+s^2\neq 0} \frac{1}{(2r-1)^{2m}+(2s-1)^{2m}}$$

$$\leq \frac{1}{2} \sum_{r^2+s^2\neq 0} \frac{1}{|2r-1|^m|2s-1|^m} < \infty, \quad \text{if } m>1,$$

so we obtain $D_1 \leq 2SN^{-2m}|u|_m^2$, where S is the sum of the series above.

As a result of (i)–(iv), we obtain

$$B \leq 2(1+4S)L^2 \mathrm{e}^{\frac{\tau}{2\delta}} N^{-2m}|u|_m^2.$$

So we obtain

$$\|I^h \mathcal{S}_{\mathcal{L}} u - \mathcal{S}_{\mathcal{L}}^h I^h u\|^2 \leq 4(5+4S)L^2|u|_m^2 \mathrm{e}^{\frac{\tau}{2\delta}} N^{-2m},$$

which leads to the expected result.   □

Now we write the discrete L^2-error estimate as the following theorem.

THEOREM 3.5. *Assume that $u_0 \in H_{\mathrm{per}}^m(\Omega)$ with $m \geq 8$ and the solution to the problem (1.1) belongs to $H^5(0,T; H_{\mathrm{per}}^m(\Omega))$. If we set $u^0 = \widetilde{U}^0 = I^h u_0$ and the condition (3.1) holds, then the discrete L^2-error at $T = n\tau$ is*

$$(3.3) \qquad \|U^n - u^n\| \leq C\left(\tau^2 + h^4 + \frac{h^m}{\tau} \right).$$

Furthermore, for the case $\tau \sim h^2$, we have

$$(3.4) \qquad \|U^n - u^n\| \leq C(\tau^2 + h^4).$$

Proof. Assume that u^{n-1}, the numerical solution at t_{n-1}-level, is given; then the discrete L^2-error at the t_n-level should be

$$(3.5) \qquad \|U^n - u^n\| \leq \|U^n - \widetilde{U}^n\| + \|\widetilde{U}^n - u^n\|.$$

The Strang splitting scheme (2.3) is second-order [27], which means that

$$\|U^n - \widetilde{U}^n\| \leq C_0 \tau^2.$$

The second term in the right-hand side of (3.5) can be bounded as follows:

$$
\begin{aligned}
\|\widetilde{U}^n - u^n\| &= \|I^h \mathcal{S}_\mathcal{L} \mathcal{S}_\mathcal{N} \mathcal{S}_\mathcal{L} \widetilde{u}^{n-1} - \mathcal{S}_\mathcal{L}^h \mathcal{S}_\mathcal{N}^h \mathcal{S}_\mathcal{L}^h u^{n-1}\| \\
&\leq \|I^h \mathcal{S}_\mathcal{L} \mathcal{S}_\mathcal{N} \mathcal{S}_\mathcal{L} \widetilde{u}^{n-1} - \mathcal{S}_\mathcal{L}^h I^h \mathcal{S}_\mathcal{N} \mathcal{S}_\mathcal{L} \widetilde{u}^{n-1}\| \\
&\quad + \|\mathcal{S}_\mathcal{L}^h I^h \mathcal{S}_\mathcal{N} \mathcal{S}_\mathcal{L} \widetilde{u}^{n-1} - \mathcal{S}_\mathcal{L}^h \mathcal{S}_\mathcal{N}^h \mathcal{S}_\mathcal{L}^h u^{n-1}\| \\
&= \|(I^h \mathcal{S}_\mathcal{L} - \mathcal{S}_\mathcal{L}^h I^h) \mathcal{S}_\mathcal{N} \mathcal{S}_\mathcal{L} \widetilde{u}^{n-1}\| + \|\mathcal{S}_\mathcal{L}^h (I^h \mathcal{S}_\mathcal{N} \mathcal{S}_\mathcal{L} \widetilde{u}^{n-1} - \mathcal{S}_\mathcal{N}^h \mathcal{S}_\mathcal{L}^h u^{n-1})\| \\
&\leq C_3 |\mathcal{S}_\mathcal{N} \mathcal{S}_\mathcal{L} \widetilde{u}^{n-1}|_m e^{\frac{\tau}{4\delta}} h^m + e^{\frac{\tau}{4\delta}} \|I^h \mathcal{S}_\mathcal{N} \mathcal{S}_\mathcal{L} \widetilde{u}^{n-1} - \mathcal{S}_\mathcal{N}^h \mathcal{S}_\mathcal{L}^h u^{n-1}\|,
\end{aligned}
$$

where the last inequality is the consequence of Lemmas 3.3 and 3.4. In addition,

$$
\begin{aligned}
\|I^h \mathcal{S}_\mathcal{N} \mathcal{S}_\mathcal{L} \widetilde{u}^{n-1} - \mathcal{S}_\mathcal{N}^h \mathcal{S}_\mathcal{L}^h u^{n-1}\| &\leq \|I^h \mathcal{S}_\mathcal{N} \mathcal{S}_\mathcal{L} \widetilde{u}^{n-1} - \mathcal{S}_\mathcal{N}^h I^h \mathcal{S}_\mathcal{L} \widetilde{u}^{n-1}\| \\
&\quad + \|\mathcal{S}_\mathcal{N}^h I^h \mathcal{S}_\mathcal{L} \widetilde{u}^{n-1} - \mathcal{S}_\mathcal{N}^h \mathcal{S}_\mathcal{L}^h u^{n-1}\| \\
&= \|(I^h \mathcal{S}_\mathcal{N} - \mathcal{S}_\mathcal{N}^h I^h) \mathcal{S}_\mathcal{L} \widetilde{u}^{n-1}\| \\
&\quad + \|\mathcal{S}_\mathcal{N}^h (I^h \mathcal{S}_\mathcal{L} \widetilde{u}^{n-1}) - \mathcal{S}_\mathcal{N}^h (\mathcal{S}_\mathcal{L}^h u^{n-1})\| \\
&\leq 3C_1 \tau (\tau^3 + h^4) + C_2 h^m + \|I^h \mathcal{S}_\mathcal{L} \widetilde{u}^{n-1} - \mathcal{S}_\mathcal{L}^h u^{n-1}\|,
\end{aligned}
$$

where the last inequality is the consequence of Lemmas 3.1 and 3.2. Furthermore,

$$
\begin{aligned}
\|I^h \mathcal{S}_\mathcal{L} \widetilde{u}^{n-1} - \mathcal{S}_\mathcal{L}^h u^{n-1}\| &\leq \|I^h \mathcal{S}_\mathcal{L} \widetilde{u}^{n-1} - \mathcal{S}_\mathcal{L}^h I^h \widetilde{u}^{n-1}\| + \|\mathcal{S}_\mathcal{L}^h I^h \widetilde{u}^{n-1} - \mathcal{S}_\mathcal{L}^h u^{n-1}\| \\
&= \|(I^h \mathcal{S}_\mathcal{L} - \mathcal{S}_\mathcal{L}^h I^h) \widetilde{u}^{n-1}\| + \|\mathcal{S}_\mathcal{L}^h (\widetilde{U}^{n-1} - u^{n-1})\| \\
&\leq C_3 |\widetilde{u}^{n-1}|_m e^{\frac{\tau}{4\delta}} h^m + e^{\frac{\tau}{4\delta}} \|\widetilde{U}^{n-1} - u^{n-1}\|,
\end{aligned}
$$

where we use the fact $\widetilde{U}^{n-1} = I^h \widetilde{u}^{n-1}$. Then we obtain

$$
\|\widetilde{U}^n - u^n\| \leq e^{\frac{\tau}{2\delta}} \|\widetilde{U}^{n-1} - u^{n-1}\| + 3C_1 e^{\frac{\tau}{4\delta}} \tau (\tau^3 + h^4) + \big(C_2 + C_3 C_T (1 + e^{\frac{\tau}{4\delta}})\big) e^{\frac{\tau}{4\delta}} h^m,
$$

where $C_T = \max\{|\mathcal{S}_\mathcal{N} \mathcal{S}_\mathcal{L} \widetilde{u}^k|_m, |\widetilde{u}^k|_m : 0 \leq k \leq n\}$. Setting $F^n = \|\widetilde{U}^n - u^n\|$ and

$$
G = 3C_1 e^{\frac{\tau}{4\delta}} (\tau^3 + h^4) + \big(C_2 + C_3 C_T (1 + e^{\frac{\tau}{4\delta}})\big) e^{\frac{\tau}{4\delta}} \frac{h^m}{\tau},
$$

we have

$$
F^n \leq e^{\frac{\tau}{2\delta}} F^{n-1} + \tau G, \quad n = 1, 2, \ldots.
$$

Using the Gronwall's lemma and the fact $e^x - 1 \geq x \ (x > 0)$, we obtain

$$
F^n \leq e^{\frac{T}{2\delta}} F^0 + \frac{\tau (e^{\frac{T}{2\delta}} - 1)}{e^{\frac{\tau}{2\delta}} - 1} G \leq e^{\frac{T}{2\delta}} F^0 + 2\delta e^{\frac{T}{2\delta}} G.
$$

Since $F^0 = \|\widetilde{U}^0 - u^0\| = 0$, we obtain

$$
\|\widetilde{U}^n - u^n\| \leq 2\delta e^{\frac{T}{2\delta}} \left(3C_1 e^{\frac{\tau}{4\delta}} (\tau^3 + h^4) + \big(C_2 + C_3 C_T (1 + e^{\frac{\tau}{4\delta}})\big) e^{\frac{\tau}{4\delta}} \frac{h^m}{\tau} \right),
$$

and thus

$$
\|U^n - u^n\| \leq C_0 \tau^2 + 2\delta e^{\frac{T}{2\delta}} \left(3C_1 e^{\frac{\tau}{4\delta}} (\tau^3 + h^4) + \big(C_2 + C_3 C_T (1 + e^{\frac{\tau}{4\delta}})\big) e^{\frac{\tau}{4\delta}} \frac{h^m}{\tau} \right).
$$

For $\tau \leq \min\{\frac{3C_{11}^2}{16A} \delta, 1\}$, we have $e^{\frac{\tau}{4\delta}} \leq e^{\frac{3C_{11}^2}{64A}} =: C_{22}$; then we obtain

$$
\|U^n - u^n\| \leq (C_0 + 6\delta e^{\frac{T}{2\delta}} C_1 C_{22}) \tau^2 + (6\delta e^{\frac{T}{2\delta}} C_1 C_{22}) h^4 + 2\delta e^{\frac{T}{2\delta}} C_{22} \big(C_2 + C_3 C_T (1 + C_{22})\big) \frac{h^m}{\tau},
$$

which implies the estimate (3.3). Furthermore, we set the step $\tau \sim h^2$ to obtain

$$\frac{h^m}{\tau} \sim h^{m-2} \sim \tau^{\frac{1}{2}m-1}.$$

Since $m \geq 8$, we obtain the error estimate (3.4). □

3.2. Accuracy tests. Now we carry out the accuracy tests on (1.1) with $\delta = 0.1$, $T = 1$, $\Omega = (0, 2\pi) \times (0, 2\pi)$, and

$$u_0(x,y) = 0.1(\sin 3x \sin 2y + \sin 5x \sin 5y),$$

which is a classical example studied either theoretically or numerically [15, 20, 22, 33]. We take the numerical solution obtained with $\tau = 5 \times 10^{-5}$ and $J = 2048$ as the "exact" solution. The tests are conducted with different spatial scales, and the time step is set to be $\tau = C_0 h^2$, where the constant C_0 is chosen to render $\tau = 0.005$ when $J = 128$. Table 1 shows the discrete L^2-errors implying an accuracy nearly $\mathcal{O}(\tau^2 + h^4)$, which is consistent with Theorem 3.5.

TABLE 1
The discrete L^2-errors with different spatial scales and time steps.

J	τ	$\|e(J)\|$	$\dfrac{\|e(J/2)\|}{\|e(J)\|}$	$\log_2 \dfrac{\|e(J/2)\|}{\|e(J)\|}$
128	5×10^{-3}	1.0278×10^{-5}	$*$	$*$
256	1.25×10^{-3}	9.5361×10^{-7}	10.7779	3.4300
512	3.125×10^{-4}	6.5869×10^{-8}	14.4774	3.8557
1024	7.8125×10^{-5}	2.4026×10^{-9}	27.4156	4.7769

4. Numerical experiments. As mentioned in section 3, a reasonable time step size τ should be controlled as order $\mathcal{O}(\delta)$. We will set $\tau = \delta/10$ in the following numerical experiments.

Example 4.1. We consider the one-dimensional epitaxial growth model

$$u_t = (u_x^3)_x - u_{xx} - \delta u_{xxxx}, \qquad (x,t) \in (0, 12) \times (0, T],$$
$$u(\cdot, t) \text{ is 12-periodic}, \qquad t \in [0, T],$$
$$u(x, 0) = 0.1 \left(\sin \frac{\pi x}{2} + \sin \frac{2\pi x}{3} + \sin \pi x \right), \quad x \in [0, 12].$$

The evolution of this initial-boundary-value problem is studied theoretically via the perturbation analysis [15] to observe the morphological instability due to the nonlinear interaction. It is also a classical example for the numerical experiments in the case $\delta = 1$. Here we will present the results obtained by the operator splitting method given in section 2. Figure 2 shows the results of the case $\delta = 1$ with $J = 128$ and $\tau = 0.1$, which is consistent with the existing work [15].

In addition, we also present some results from reducing δ to 0.1, 0.01, and 0.001, respectively. The results are summarized in Figures 3–5. The first plot in each figure presents the height $u(x, t)$ at some time t, the second one shows the corresponding gradient $u_x(x, t)$, and the third one plots the evolution of the energy $E(u(\cdot, t))$.

Figure 3 presents the results of the case $\delta = 0.1$ with $(J, \tau) = (128, 0.01)$ and $(J, \tau) = (256, 0.005)$. We find that both solutions have few differences between them, so we are convinced that the results presented here are credible. The energy decreases
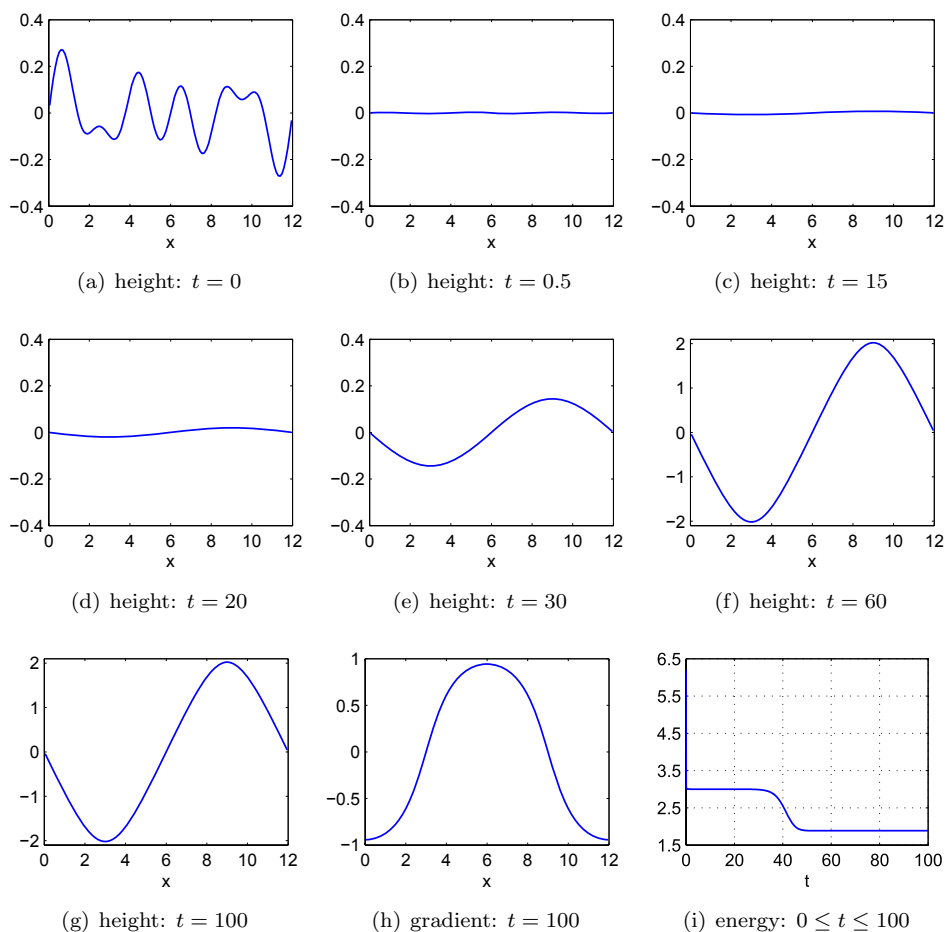
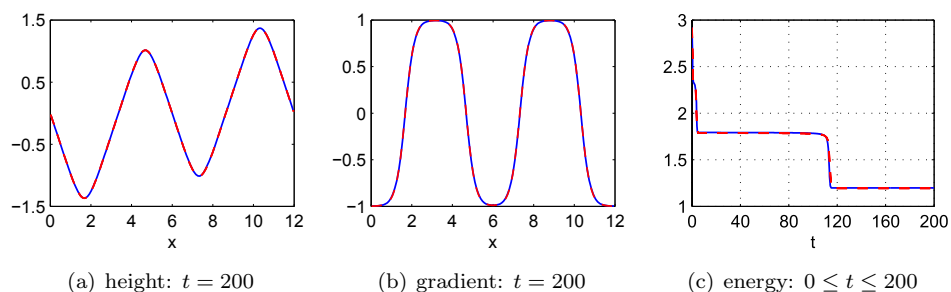FIG. 2. *Example* 4.1: *The results of the case* $\delta = 1$.

FIG. 3. *Example* 4.1: *The results of the case* $\delta = 0.1$ *obtained with* $(J, \tau) = (128, 0.01)$ *(solid line) and* $(J, \tau) = (256, 0.005)$ *(dashed line)*.

little after $t = 200$ so that we view the solution at $t = 200$ as the steady state. It is observed from the left and middle graphs that there are two complete waves in the steady state whose gradients do not exceed the range between -1 and 1.
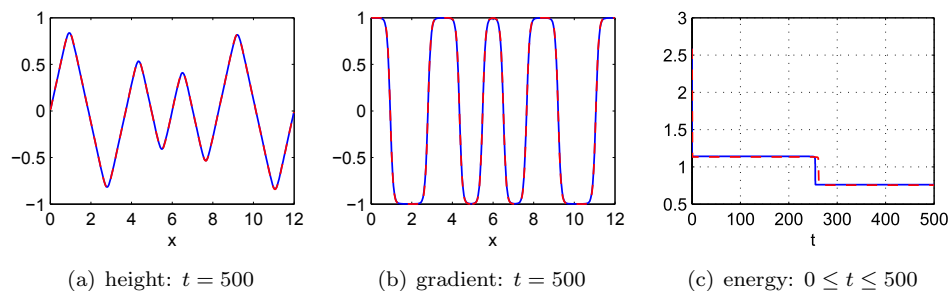
(a) height: $t = 500$ (b) gradient: $t = 500$ (c) energy: $0 \le t \le 500$

FIG. 4. *Example* 4.1*: The results of the case* $\delta = 0.01$ *obtained with* $(J, \tau) = (256, 0.001)$ *(solid line) and* $(J, \tau) = (512, 0.0005)$ *(dashed line).*
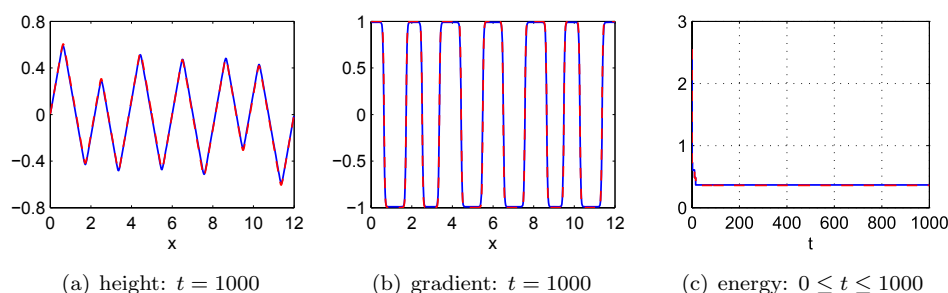

(a) height: $t = 1000$ (b) gradient: $t = 1000$ (c) energy: $0 \le t \le 1000$

FIG. 5. *Example* 4.1*: The results of the case* $\delta = 0.001$ *obtained with* $(J, \tau) = (512, 0.0001)$ *(solid line) and* $(J, \tau) = (1024, 0.00005)$ *(dashed line).*

Figure 4 gives the results of the case $\delta = 0.01$ with $(J, \tau) = (256, 0.001)$ and $(J, \tau) = (512, 0.0005)$. Figure 5 gives the results of the case $\delta = 0.001$ with $(J, \tau) = (512, 0.0001)$ and $(J, \tau) = (1024, 0.00005)$. Likewise, we can trust these results. The solutions at the steady states present more waves in the considered domain than those above, and the gradients still locate in the interval $[-1, 1]$.

From the gradient graphs of Figures 2–5, we find that the smaller δ is, the more points on the gradient curves locate at the horizon lines $y = 1$ or $y = -1$. This is a consequence of the competitions between the Ehrlich–Schwoebel effect and the dissipation mechanism of the energy functional

$$E(u) = \int_0^{2L} \left(\frac{1}{4}(u_x^2 - 1)^2 + \frac{\delta}{2} u_{xx}^2 \right) \, \mathrm{d}x.$$

It is seen that the Ehrlich–Schwoebel effect selects the slope $|u_x| = 1$ while the dissipation term weakens the selection. To reduce δ means to weaken the dissipation effect or, equivalently, to strengthen the slope selection. And thus, the gradient interfaces connecting -1 to 1 turn steep and the solution curves turn sharp there.

Example 4.2 (coarsening dynamics). We simulate the two-dimensional epitaxial growth model (1.1) with $\delta = 0.1$ on the domain $\Omega = (0, 100) \times (0, 100)$ with a 512×512 grid. We set the initial data as a stochastic state by a random number varying from -0.001 to 0.001 on each grid point. The time step is set to be $\tau = 0.01$.

This example is intended to verify the power laws for the energy evolution and the height growth.
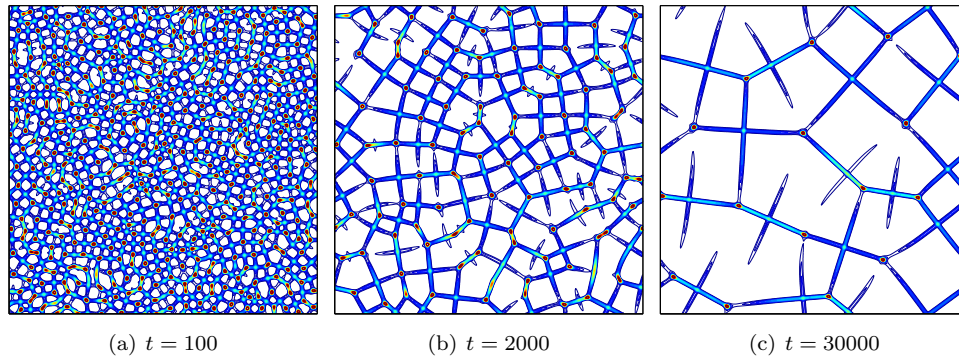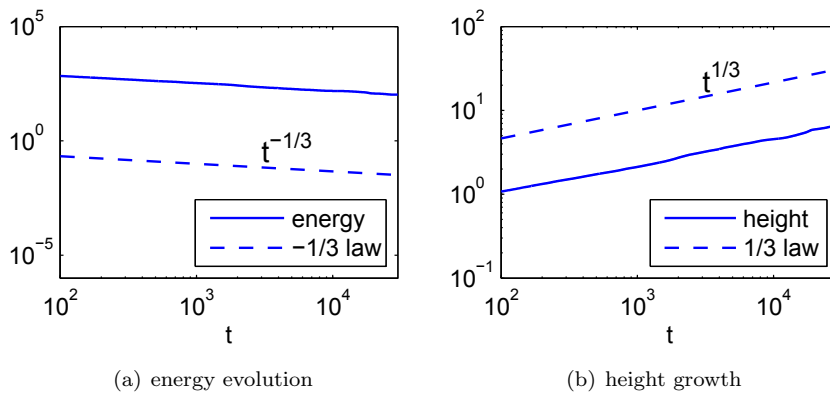
(a) $t = 100$ (b) $t = 2000$ (c) $t = 30000$

FIG. 6. *Example 4.2: Contour lines of the free energy F_{free}.*

(a) energy evolution   (b) height growth

FIG. 7. *Example 4.2: The power law for the evolution of the energy and the interface height.*

Figure 6 presents the contour lines of the free energy

$$F_{\text{free}} := \frac{1}{4}(|\nabla u|^2 - 1)^2 + \frac{\delta}{2}|\Delta u|^2$$

at $t = 100$, 2000, and 30000.

Figure 7 shows the evolution of the energy and the interface height. Panel (a) presents the power law for the evolution of the energy. The energy curve is plotted in log-to-log scale and nearly parallels to the dashed line $t^{-\frac{1}{3}}$, which suggests that the energy evolves in time as the power law Ct^α with $\alpha \approx -\frac{1}{3}$. Panel (b) presents the power law for the growth of the interface height $h(t)$, which is defined by

$$h(t) = \left(\frac{1}{|\Omega|} \int_\Omega u^2(x, y, t)\, \mathrm{d}x\mathrm{d}y \right)^{\frac{1}{2}}.$$

Again, the height curve is plotted in log-to-log scale. The growth of the interface height approximately obeys the power law Ct^β with $\beta \approx \frac{1}{3}$, which is consistent with the existing works (see, e.g., [20, 22, 33]).

5. Conclusions. In this work, we investigate the error estimate of an FEOS method for a nonlinear fourth-order diffusion equation modeling epitaxial growth

of thin films. The convergence order $\mathcal{O}(\tau^2 + h^4)$ in discrete L^2-norm is proved theoretically and verified numerically. For the nonlinear subproblem, we construct a 25-point center-difference scheme in space and use the third-order explicit SSP-RK3 scheme in time. Since fewer points are involved in the scheme at each node compared to the 33-point center-difference scheme presented in [1], the restriction for the stability may be reduced. We carry out several numerical experiments to verify the efficiency of the derived algorithm and present some results for small δ's with the time step $\tau = \delta/10$. Furthermore, we find numerically the coarsening exponents for the energy evolution and the height growth are $-1/3$ and $1/3$, respectively.

REFERENCES

[1] Y. Z. Cheng, A. Kurganov, Z. L. Qu, and T. Tang, *Fast and stable explicit operator splitting methods for phase-field models*, J. Comput. Phys., 303 (2015), pp. 45–65.

[2] A. Chertock and A. Kurganov, *On splitting-based numerical methods for convection-diffusion equations*, in Numerical Methods for Balance Laws, Quad. Mat. 24, Seconda Universitá degli Studi di Napoli, Caserta, Italy, 2009, pp. 303–343.

[3] A. Chertock, A. Kurganov, and G. Petrova, *Fast explicit operator splitting method. Application to the polymer system*, in Finite Volumes for Complex Applications IV, ISTE, London, 2005, pp. 63–72.

[4] A. Chertock, A. Kurganov, and G. Petrova, *Fast explicit operator splitting method for convection-diffusion equations*, Int. J. Numer. Methods Fluids, 59 (2009), pp. 309–332.

[5] G. Ehrlich and F. G. Hudda, *Atomic view of surface self-diffusion: Tungsten on tungsten*, J. Chem. Phys., 44 (1966), pp. 1039–1049.

[6] J. W. Evans, P. A. Thiel, and M. C. Bartelt, *Morphological evolution during epitaxial thin film growth: Formation of 2D islands and 3D mounds*, Surf. Sci. Rep., 61 (2006), pp. 1–128.

[7] D. J. Eyre, *Unconditionally gradient stable time marching the Cahn-Hilliard equation*, in Computational and Mathematical Models of Microstructural Evolution, Mater. Res. Soc. Symp. Proc. 529, J. W. Bullard, R. Kalia, M. Stoneham, and L. Q. Chen, eds., Materials Research Society, Warrendale, PA, 1998, pp. 39–46.

[8] S. Gottlieb, C.-W. Shu, and E. Tadmor, *Strong stability preserving high-order time discretization methods*, SIAM Rev., 43 (2001), pp. 89–112.

[9] S. Gottlieb and C. Wang, *Stability and convergence analysis of fully discrete Fourier collocation spectral method for 3-D viscous Burgers' equation*, J. Sci. Comput., 53 (2012), pp. 102–128.

[10] M. A. Herman and H. Sitter, *Molecular Beam Epitaxy: Fundamentals and Current Status*, Springer-Verlag, Berlin, 1989.

[11] C.-Y. Kao, A. Kurganov, Z. L. Qu, and Y. Wang, *A fast explicit operator splitting method for modified Buckley-Leverett equations*, J. Sci. Comput., 64 (2015), pp. 837–857.

[12] R. V. Kohn and X. Yan, *Upper bound on the coarsening rate for an epitaxial growth model*, Commun. Pure Appl. Math., 56 (2003), pp. 1549–1564.

[13] A. Kurganov and D. Levy, *A third-order semidiscrete central scheme for conservation laws and convection-diffusion equations*, SIAM J. Sci. Comput., 22 (2000), pp. 1461–1488.

[14] H. G. Lee, J. Shin, and J.-Y. Lee, *First and second order operator splitting methods for the phase field crystal equation*, J. Comput. Phys., 299 (2015), pp. 82–91.

[15] B. Li and J.-G. Liu, *Thin film epitaxy with or without slope selection*, European J. Appl. Math., 14 (2003), pp. 713–743.

[16] D. Li, Z. H. Qiao, and T. Tang, *Characterizing the stabilization size for semi-implicit Fourier-spectral method to phase field equations*, SIAM J. Numer. Anal., 54 (2016), pp. 1653-1681.

[17] S. Mishra and M. Svärd, *On stability of numerical schemes via frozen coefficients and the magnetic induction equations*, BIT, 50 (2010), pp. 85–108.

[18] D. Moldovan and L. Golubovic, *Interfacial coarsening dynamics in epitaxial growth with slope selection*, Phys. Rev. E, 61 (2000), pp. 6190–6214.

[19] Z. H. QIAO AND S. Y. SUN, *Two-phase fluid simulation using a diffuse interface model with Peng-Robinson equation of state*, SIAM J. Sci. Comput., 36 (2014), pp. B708–B728.
[20] Z. H. QIAO, Z. Z. SUN, AND Z. R. ZHANG, *The stability and convergence of two linearized finite difference schemes for the nonlinear epitaxial growth model*, Numer. Methods Partial Differential Equations, 28 (2012), pp. 1893–1915.
[21] Z. H. QIAO, T. TANG, AND H. H. XIE, *Error analysis of a mixed finite element method for the molecular beam epitaxy model*, SIAM J. Numer. Anal., 53 (2015), pp. 184–205.
[22] Z. H. QIAO, Z. R. ZHANG, AND T. TANG, *An adaptive time-stepping strategy for the molecular beam epitaxy models*, SIAM J. Sci. Comput., 33 (2011), pp. 1395–1414.
[23] R. L. SCHWOEBEL AND E. J. SHIPSEY, *Step motion on crystal surfaces*, J. Appl. Phys., 37 (1966), pp. 3682–3686.
[24] J. SHEN AND T. TANG, *Spectral and High-Order Methods with Applications*, Science Press, Beijing, 2006.
[25] J. SHEN, T. TANG, AND L. L. WANG, *Spectral Methods: Algorithms, Analysis and Applications*, Springer, Berlin, 2011.
[26] J. SHEN, C. WANG, X. M. WANG, AND S. M. WISE, *Second-order convex splitting schemes for gradient flows with Ehrlich-Schwoebel type energy: Application to thin film epitaxy*, SIAM J. Numer. Anal., 50 (2012), pp. 105–125.
[27] G. STRANG, *On the construction and comparison of difference schemes*, SIAM J. Numer. Anal., 5 (1968), pp. 506–517.
[28] Z. Z. SUN, *The Method of Order Reduction and Its Application to the Numerical Solutions of Partial Differential Equations*, Science Press, Beijing, 2009.
[29] L. N. TREFETHEN, *Spectral Methods in MATLAB*, SIAM, Philadelphia, 2000.
[30] C. WANG, X. M. WANG, AND S. M. WISE, *Unconditionally stable schemes for equations of thin film epitaxy*, Discrete Contin. Dyn. Syst. Ser. A, 28 (2010), pp. 405–423.
[31] C. WANG AND S. M. WISE, *An energy stable and convergent finite-difference scheme for the modified phase field crystal equation*, SIAM J. Numer. Anal., 49 (2011), pp. 945–969.
[32] S. M. WISE, C. WANG, AND J. S. LOWENGRUB, *An energy-stable and convergent finite-difference scheme for the phase field crystal equaiton*, SIAM J. Numer. Anal., 47 (2009), pp. 2269–2288.
[33] C. J. XU AND T. TANG, *Stability analysis of large time-stepping methods for epitaxial growth models*, SIAM J. Numer. Anal., 44 (2006), pp. 1759–1779.